



27th International Conference on Flexible Automation and Intelligent Manufacturing, FAIM2017,  
27-30 June 2017, Modena, Italy

## Optical tactile probe for the inspection of mechanical components

Sandro Barone<sup>a</sup>, Paolo Neri<sup>a,\*</sup>, Alessandro Paoli<sup>a</sup>, Armando Razionale<sup>a</sup>

<sup>a</sup>University of Pisa, Largo L. Lazzarino 1, Pisa 56122, Italy

---

### Abstract

Mechanical components are often subjected to tolerances and geometrical specification. This paper describes an automatic 3D measurement system based on the integration of a stereo structured light scanner and a tactile probe. The tactile probe is optically tracked by the optical scanner by means of 3D measurements of a prismatic flag, rigidly connected to the probe and equipped with multiple chessboard patterns. Both the stereo vision system and the tactile probe can be easily configured enabling complete reconstructions of components having complex shapes. For instance, structured light scanning can be used to acquire external and visible geometries while tactile probing can be limited to the acquisition of internal and hidden surfaces.

© 2017 The Authors. Published by Elsevier B.V. This is an open access article under the CC BY-NC-ND license (<http://creativecommons.org/licenses/by-nc-nd/4.0/>).

Peer-review under responsibility of the scientific committee of the 27th International Conference on Flexible Automation and Intelligent Manufacturing.

*Keywords:* Optical touch probe; Geometrical inspection; Reverse Engineering

---

### 1. Introduction

Reverse Engineering (RE) techniques [1] are widely used in all branches of modern manufacturing industry. In the field of mechanical engineering and industrial manufacturing, RE refers to the creation of geometrical documentation data from existing physical parts [2]. With the rapid development of Computer Aided Design (CAD), Computer Aided Manufacturing (CAM) and Computer Aided Engineering (CAE) technologies, RE technology has become a significant tool to shorten the product development cycle. When original drawings are not available, it is

---

\* Corresponding author. Tel.: +39-050-2218019; fax: +39-050-2218069.  
E-mail address: [paolo.neri@dici.unipi.it](mailto:paolo.neri@dici.unipi.it)

often required to reconstruct CAD models from the existing parts by exploiting digitization techniques. These models can be used to optimize the design process through numerical analyses in order to improve the product effectiveness. Moreover, 3D printing, one the most representative technologies for Industry 4.0, can be adopted to generate components directly from CAD data in a very short time, thus defining more efficient, value-added manufacturing processes.

In general, the shape of an existing physical model can be retrieved by using contact or non-contact measuring devices. Traditional point-by-point systems, as mechanical probes, or full-field optical scanners may be adopted to acquire target surfaces even characterized by complex geometries. Coordinate Measuring Machines (CMMs) with contact probes provide measurements with high accuracies [3]. However, on-site measurements are not allowed due to the bulky equipment, which is usually restricted in dedicated measurement rooms. Articulated arms, characterized by 6 or 7 DoF, can be alternatively used [4]. These systems, equipped with either a laser line scanner or a touch probe, can be manually moved with respect to the target object and may result particularly effective for on-site measurements. The main drawback of CMMs and articulated arms is that they only provide a limited number of sampling points and are not suitable if free-from shapes must be reconstructed. Among non-contact approaches, optical methods based on the triangulation principle are able to provide full-field measurements with minimal interaction with the operator. Laser line scanning and structured light scanning can be indifferently used to obtain dense point cloud data on the measured surfaces [5]. Marker-based systems are also used in practical applications [6] but suffer the same limitation in the number of acquired points.

All the above-described approaches, however, have inherent limitations in the reconstruction of complex surfaces. Optical techniques allow the acquisition of visible surfaces, whereas the digitization of internal geometries (i.e., slot, holes) is subjected to partial or complete restrictions due to optical occlusions. Tactile probing methods are hampered by the cumbersomeness of the equipment (CMMs), which lowers flexibility and portability, and/or kinematic of the linkage structure (articulated arms) which limits the ergonomics of the process thus preventing the acquisition of complex hidden geometries. For this reason, complete reconstructions providing visible and internal geometries should be obtained by integrating contact and non-contact methodologies.

In this paper, an automatic and versatile 3D measurement system has been developed by integrating tactile and optical probing. In particular, a hand-held tactile probe and a stereo structured light scanner are combined with the aim at performing reliable multi-sensor measurements of mechanical components. The tactile probe is optically tracked by the stereo camera system of the optical scanner by means of 3D measurements of a prismatic flag, rigidly connected to the probe, and equipped with multiple chessboard patterns differentiated by a QR code. The probe configuration has been designed to provide both versatility and adaptability to various applicative contexts. The adoption of multiple planar surfaces reduces the stereo occlusion problem thus increasing the number of tracked points always visible by the stereo vision system in spite of the hand orientation. Moreover, a suitable calibration process has been developed by exploiting the structured light scanner in order to relate the probe tip with respect to the tracking flag. A wireless control of the stereo cameras has been implemented with the aim at enhancing the ergonomics of the tactile probing process since the operator may accomplish the measurements without removing the hand from the probe handle. Although some commercial solutions of optically tracked touch probes have been proposed [7-9], their effectiveness in the reconstruction of actual industrial parts has not yet been fully evidenced. Moreover, the designed multi-sensor system allows the integration of full-field optical measurements of visible surfaces with point-by-point contact measurements performed by the hand-held tactile probe. The geometry of the probe stylus is designed in order to allow the probing of non-visible internal surfaces, making possible complete reconstructions of components having complex shape. The whole system has been developed with the aim at carrying out on-site measurements even in non-collaborative environments, thus bypassing typical limitations of CMMs and articulated arms. The effectiveness of the proposed solution has been finally tested in the acquisition of mechanical components.

## 2. Proposed approach

The proposed approach is based on the integration of a stereo structured light scanner with a hand-held touch probe (Fig. 1). The overall measurement tool is based on the stereo triangulation principle. When a scene is acquired by two independent and calibrated cameras, it is possible to determine the 3D coordinates of each point in the scene

starting from the 2D coordinates of the correspondent points in the two acquired images (left and right images). The critical issue of this approach is represented by the stereo-matching problem. For each point on the left image, the corresponding point on the right image must be determined. In this work, the stereo matching problem has been faced by following two different strategies. The optical scanner has been assembled by exploiting an active approach since it uses a multimedia projector to project a sequence of vertical and horizontal light stripes. In particular, a multi-temporal Gray Code Phase Shift Profilometry (GCPSP) method is used to encode and reconstruct the scene [10]. This methodology solves the stereo matching problem by encoding  $l_v \times l_h$  points, where  $l_v$  and  $l_h$  are the numbers of vertical and horizontal lines switched by the projector, respectively. The two cameras of the optical scanner are also used to optically track the hand-held touch probe. In this case, the stereo matching problem is faced by using specific patterns (*chessboard patterns*), which are automatically recognized in the camera images. At this purpose, the probe has been configured with a flag (*optical tracking flag*) holding the aforementioned patterns. The flag shape is designed in order to improve its visibility in spite of the hand orientation. The touch probe is composed of a supporting arm and a sharp tip, which can be used to measure also surfaces presenting accessibility restrictions. The measurement of the points characterizing the pattern on the flag, however, does not directly provide the coordinates of the tip vertex. For this reason, a calibration process must be accomplished before the measurement stage in order to geometrically relate the probe tip with respect to the tracking flag. This approach allows an accurate estimation of the probe tip coordinates even if the tip vertex is not directly visible by the cameras and then not measurable by the structured light scanner.

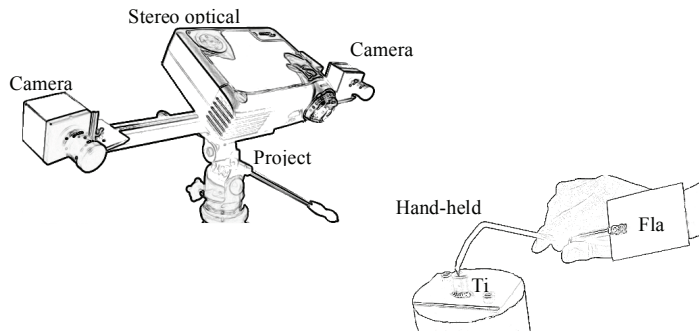


Fig. 1. Overall system set-up.

### 2.1. Hardware set-up

The stereo optical scanner is composed of two monochrome CCD digital cameras ( $1600 \times 1200$  pixels), equipped with 16 mm focal lenses, and a DLP white light projector ( $1024 \times 768$  pixels), Fig. 2. The stereo rig is calibrated by evaluating the intrinsic and the extrinsic parameters of the vision devices.



Fig. 2. 3D Optical scanner composed of two digital cameras and a multimedia projector.

The touch probe has been developed in order to take into account ergonomic factors. The overall design must guarantee a stable probe handling during acquisitions, so that the flag could appear still during the measurement process. A wireless acquisition control system has been also implemented and housed within the handle to further facilitate the operations. Several distinct parts have been assembled (Fig. 3):

- Sharp tip vertex;
- Tip support;
- Handle;
- Electronic control unit.
- Optical tracking flag;

The mere probing part is composed by a sharp tip vertex, created with the aim at accurately defining the measurement point, and a stem, which is welded to the main shaft (green color in Fig. 3). The shaft is then joined to a supporting plate (purple color in Fig. 3), by threaded connections. The plate connects the touch probe to the handle (orange color in Fig. 3), which has been designed in order to contain the electronic control unit. The handle shape has been studied with particular attention to the ergonomics and manufactured by 3D printing (Fig. 4a). It was divided in two halves, to facilitate the 3D printing process and the electronics mounting procedure (Fig. 4b). Weight reduction represents a primary requirement since one-hand operations are to be preferred to enhance manoeuvrability. Brass inserts are glued in the printed holes of the handle, thus providing stable and durable mechanical connections at bolts level.

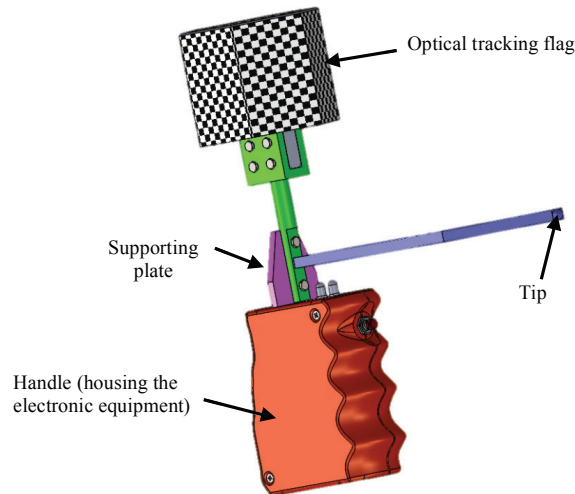


Fig. 3. Touch probe CAD model.

A signal is required to control and synchronize the stereo cameras since the 3D measurements need images acquired by two different orientations at the same time. At this purpose, a wireless system, controlled by a push button introduced in the handle, was selected in order to avoid cables thus improving the ease of handling. A simple and reliable configuration, consisting in a Radio Frequency (RF) emitter and transmitter couple, which operates at 433 MHz, was chosen. The electronic control of the system was achieved through Arduino boards: an Arduino NANO board was embedded in the handle and an Arduino UNO board was used to receive the signal and to communicate with the software, which drives the cameras and performs the image elaboration task (see next section). A 17 cm antenna was mounted on both transmitter and receiver to enhance the transmission signal, so that a 10 m transmission range could be achieved. A custom circuit was also embedded in the handle to command some leds, the device switch and the transmitter connection with the Arduino NANO board. The program controlling the

Arduino NANO board was downloaded by the transmitter supplier website and slightly modified to control the acquisition feedback led. The program on the Arduino UNO board was developed to read the signal produced by the receiver and to convert it into a software signal, which is sent to the control PC. The cameras were connected to a common trigger, in order to continuously obtain synchronized frames. Then, when the acquisition signal arrives from the RF transmitter, the frames acquired by the cameras were stored in memory for later post-processing.

The main probe shaft is also connected to the optical tracking flag. A relevant design effort was spent in the flag definition, in order to simplify the measuring process. Preliminary design solutions considered the use of few markers randomly placed on a plane flag [11, 12]. However, this simple approach limits the flexibility of the process since the plate must be always placed in front of the two cameras during the measurement stage. For this reason, in this work, a multi-planar flag has been designed. In particular, the use of a hexagonal prismatic shape, characterized by six rectangular lateral faces and a hexagonal superior face, guarantees that at least one of the faces is always visible by the stereo system regardless the hand orientation (Fig. 4c). The number of the prismatic faces has been determined as a tradeoff between the need to keep adequate planar dimensions for each pattern without excessively lowering the angle between two adjacent faces (visibility issues). A specific pattern was then attached to each of the flag facets and used to optically track the probe placements.

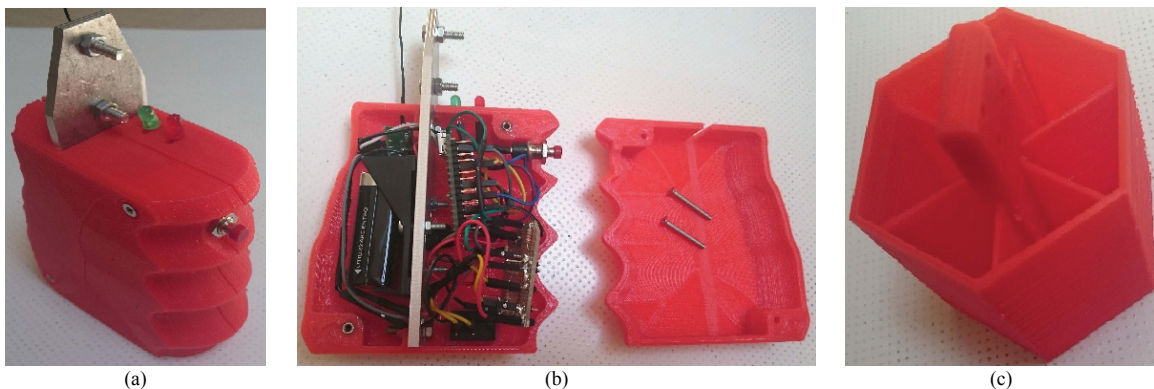


Fig. 4. 3D printed parts: (a) assembled handle, (b) electronics housed within the handle and (c) hexagonal prismatic flag.

## 2.2. Optical tracking pattern

Fig. 5 shows, as an example, two patterns printed on two distinct faces of the prismatic flag. The pattern is composed by three distinct elements: 1) three QR code markers, 2) a chessboard pattern and 3) a numbering bar. The QR code markers are placed at the corners of the rectangular face in order to define the area containing the chessboard pattern and to provide X and Y directions. The central chessboard pattern, having 3.8 mm edges, is used to define a point grid structure: the chess corners are automatically detected and used to determine the actual measurement points. The lateral numbering bar is finally used to discriminate the face captured by the cameras among all the seven prismatic facets. A high contrast narrow edge is used to delimit the *active* area that must be processed by the tracking algorithm.

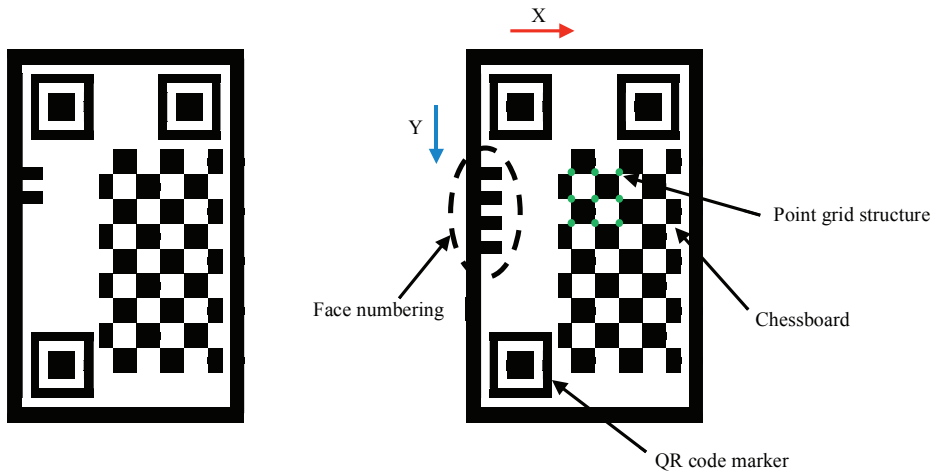


Fig. 5. Two examples of the optical tracking pattern.

### 3. 3D measurement process

The 3D measurement process integrates full field acquisitions in the form of point clouds with point-by-point acquisitions carried out by the tactile probe. In this context, the structured light scanner has a twofold function: 1) reconstructing visible geometries by triangulating encoded light patterns provided by the light projector and reflected by the target object, 2) defining a structured light procedure to calibrate the touch probe (i.e., relating the tip vertex coordinates with respect to the flag point grid structures). If the stereo camera system is kept fixed with respect to the component during the whole measurement, both full-field point clouds and tactile probed points are expressed in the same reference system and can be directly integrated.

#### 3.1. Image processing for the flag tracking

The crucial issue in the probe placement detection is the automatic recognition of at least one point grid structure in both left and right images, in order to solve the stereo-matching problem and compute the 3D coordinates of the acquired points. The tracking algorithm has been then divided into sequential steps. Firstly, a binarization process is performed on the basis of a threshold level, which depends on the ambient light intensity and faces orientation. This threshold value can be manually selected or iteratively determined. The QR code markers detection is carried out on the binarized image. Each QR code marker has a known proportion of black and white regions along all the direction passing by the marker center. More precisely, black and white repetitions are in the proportion of 1-1-3-1-1, as shown in Fig. 6a. The whole image is then analyzed to detect regions respecting this black/white proportion, denoting the presence of a marker. At the end of this step, the total number of markers detected in each image is three times the number of visible flag faces, and a list of marker centers can be obtained. As visible in Fig. 6b, X and Y axes are defined on each face by markers having different relative distances. All the combinations of the available markers are three to three tested to check if the proportion between the (possible) X and Y axes respects the known proportion of Fig. 6b. In this way, the full set of markers is divided into subsets containing three markers, each defining a Cartesian frame. Once the coordinates of the origin O and the orientation of the Y-axis are known, it is possible to compute the black bands on the numbering bar placed on the left side of the pattern, in order to univocally identify the flag face.

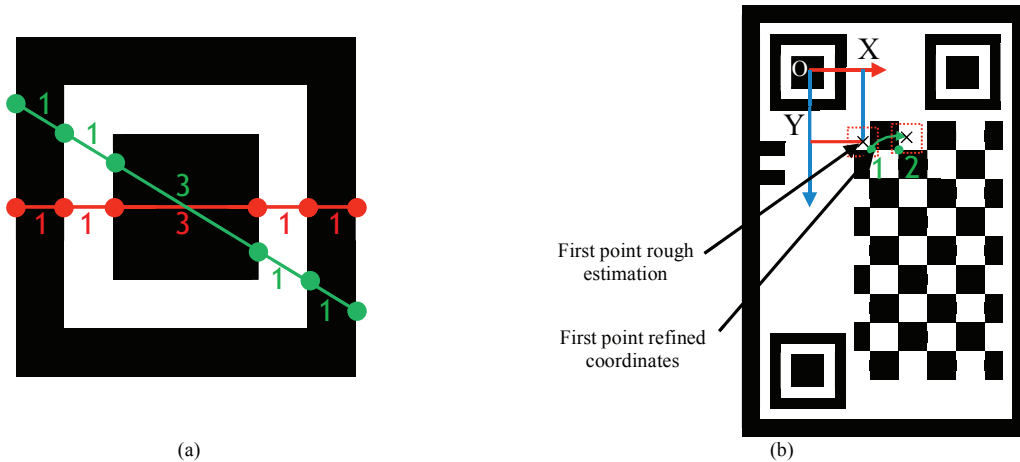


Fig. 6. a) QR code marker: black and white alternation scheme, b) chessboard corner detection procedure.

All this information is not directly related to the grid point structure and do not require a high accuracy. The last step regards the detection of the chessboard corners (grid point structure), which instead requires a sub-pixel accuracy. The coordinates of the origin  $O$  are used to provide a first estimate of the first point in the grid, while a corner-finder algorithm is used to refine the initial rough estimation. Thus, the whole grid structure is iteratively determined starting from the exact coordinates of the first point and proceeding for each successive point with the same coarse-fine approach. Fig. 6b shows a scheme of this iterative process. The described procedure provides the coordinates of the point grid structure as well as the face to which these points belong. It is worth noting that it is possible to detect, within the same image, distinct grid point structures belonging to different faces, depending on the threshold level used for the binarization process. For this reason, the grid point detection is repeated with different threshold values and all the detected point structures are stored. The described approach is carried out on both left and right images in order to ascertain which faces are properly detected by both cameras. Preliminary tests showed that a maximum of three distinct flag faces are detectable in each single image, while only a maximum of two distinct flag faces are simultaneously detectable by both cameras. The most common case, anyway, is represented by a single face being simultaneously detected by both cameras. It is worth noting that the above-described procedure (schematized in Fig. 6b) detects points following the same order for both left and right images. Thus, the stereo-matching problem is automatically solved and the stereo-triangulation process is straightforward. The grid point detection succeeds or fails only depending on the Cartesian frame determination. In some cases, the algorithm can properly detect QR code markers and Cartesian frame, but a significant error results in the point grid determination. This issue may occur, for example, if a flag face is viewed with a relevant angle by one of the two cameras, or if spotlights are present in the images. A further development of the algorithm is then represented by a grid-quality evaluation. A good-quality grid is characterized by two main aspects: the point alignment inside the grid (i.e. parallelism of rows and columns) and the equidistance between grid points. An automatic feedback algorithm was then developed to evaluate these two properties and determine if the grid can be effectively used for metrology purposes. This real-time control allows the operator to understand if the probing measurement process is successful and to modify the probe orientation if the point grid structure is not reconstructed with the required accuracy. Fig. 7 and 8 show two examples of the point grid structure detection on left and right images of the stereo camera pair. In Fig. 7, the grid of one of the seven faces (face 3) is correctly detected in both images (and then visualized by overlapping green dots on the relative chessboard). As can be observed, the grid structure placed on face 4 is detected only on the right image (due to the high viewing angle of this prismatic facet with respect to the left camera); hence, it cannot be used for the measurement process. On the other hand, Fig. 8 reports a case with the point grid structure on the fourth facet properly detected only on the left image and the point grid structure on the third facet incorrectly detected only on the right image (overlapped red dots on the relative chessboard). In this latter scenario, the same point grid structure on both left and right images was not detected, thus preventing the stereo-

triangulation process. A great amount of possible false positive elements was intentionally added in the background scene, as visible in Fig. 7 and 8, in order to assess the algorithm robustness.

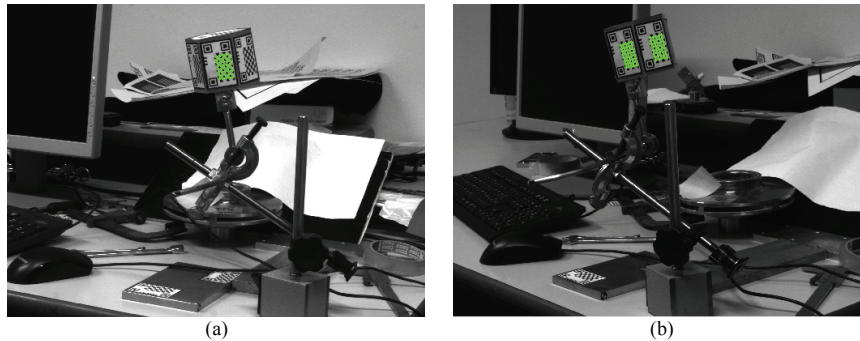


Fig. 7. Point grid structure properly detected by the software both in left (a) and right image (b).

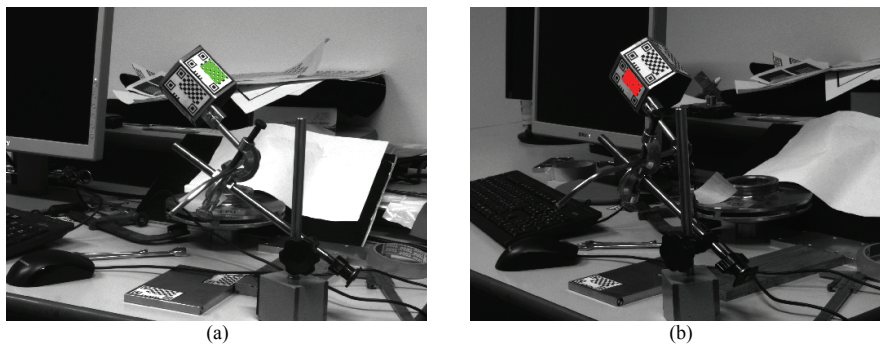


Fig. 8. Point grid structure properly detected by the software in the left image (a) but not in the right image (b).

A measurement campaign was performed with various flag orientations (100 acquisitions) to assess the algorithm performance in terms of tracking capabilities. At least one facet of the flag was always detected by the algorithm, provided that camera settings are adequate with respect to room illumination. The grid-quality evaluation algorithm shown a 93% of good quality grids detection.

### 3.2. Touch probe calibration

The measurement of the point grids on the probe flag, however, does not directly provide the coordinate of the tip vertex, which physically performs the contact measurement. For this reason, a calibration process must be carried out in order to relate the probe tip coordinates with respect to the point grid structure of each hexagonal flag facet. This calibration procedure must be done before the measurement stage and does not need to be repeated unless a relative displacement between the flag and the tip occurs (accidental impact or device wear). The developed procedure, which calibrates each face singularly, is based on the acquisition of a reference plane by both the tactile probe and the structured light scanner. The tactile probe is placed and fixed within the working volume so that the flag facet to be calibrated is properly visible by both cameras. A reference planar surface is then placed in the working volume in contact with the probe tip vertex and acquired by the structured light scanner, as shown in Fig. 9. Thus, a point cloud representing the planar surface is obtained in the camera's reference system. The point grid structure of the considered flag facet is also detected and triangulated with the above-described approach. This procedure is repeated for three different orientations of the reference planar surface with the probe tip kept always fixed and in contact with the plane. It is then possible to determine the 3D coordinates of the tip vertex by determining the intersection between the three planes acquired by the optical scanner. Hence, probe tip coordinates and grid coordinates are known in the same reference system and can be stored as a calibration parameter. The



optical stereo system must be fixed for the whole calibration procedure and can be moved only when another hexagonal facet is calibrated. The described procedure is repeated for all the flag facets. During the measurement process, it is then possible to determine the tip placement by acquiring the point grid structures and using the corresponding calibration information.

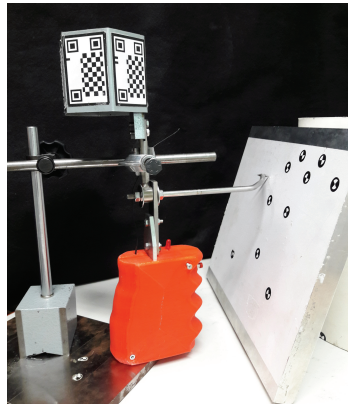


Fig. 9. Calibration setup: example of plane acquisition.

#### 4. Results

The tactile probe has been used to measure the surface of a propeller blade (Fig. 10a). Firstly, a full-field structured light acquisition was performed, in order to have a reference surface for comparison purposes. The structured light scanner used for the acquisition of the reference surface has an accuracy of 0.05 mm. Secondly, 27 points were acquired by the tactile probe on the same blade region reconstructed by the structured light scanner. These punctual measurements were compared to the structured light results, in order to evaluate the discrepancies between the two datasets. Finally, 32 further points were acquired by the tactile probe on a blade region not visible by the 3D scanner due to optical undercuts. Results are reported in Fig. 10b: the grey surface represents the tessellated model obtained by the full-field point cloud; red circles represent the points probed by the tactile device for comparison purposes, while black crosses represent the points probed by the tactile device in correspondence of not visible areas. Further data elaboration has denoted a mean distance between the probed points and reference surface of 0.2 mm and a standard deviation of 0.114 mm.

#### 5. Conclusions

The presented research activity has been focused on the design of a tactile probe to be used for the geometrical inspection of mechanical components. In particular, an integration between a full-field optical scanner, based on a structured light approach, and a tactile probe has been developed with the aim at creating a measurement system, which can be adapted to various industrial environments. The stereo camera pair of the 3D scanner is used to optically track the tactile probe, thus allowing the integration of point-by-point measurements in the same reference frame of the full-field scans. Both the stereo vision system and the tactile probe can be easily configured enabling complete reconstructions of components having complex shapes. For instance, structured light scanning can be used to acquire external and visible geometries while the more time consuming tactile probing process can be limited to the acquisition of internal and hidden surfaces. Preliminary results showed an adequate robustness of the device as well as an ease of use, giving a measurement error in the order of 0.2 mm (which could be easily reduced by using higher resolution cameras).

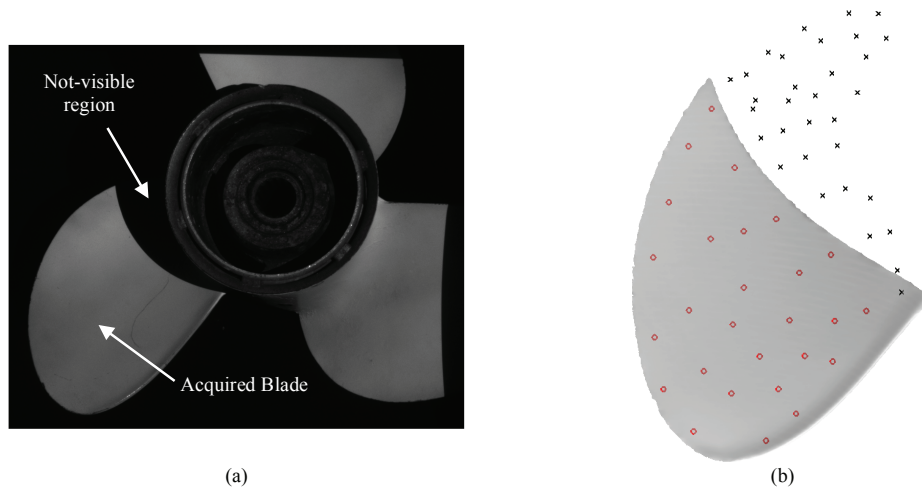


Fig. 10. Tactile probe case study: (a) acquired blade and (b) integration between full-field and point-by-point tactile measurements.

## References

- [1] T. Varady, R.R. Martin, J. Cox, Reverse engineering of geometric models - An introduction, *Comput Aided Design*, 29 (1997) 255-268.
- [2] V. Raja, K.J. Fernandes, *Reverse Engineering: an Industrial Perspective*, Springer London 2008.
- [3] A. Weckenmann, T. Estler, G. Peggs, D. McMurtry, Probing systems in dimensional metrology, *Cirp Ann-Manuf Techn*, 53 (2004) 657-684.
- [4] F. Romdhani, F. Hennebelle, M. Ge, P. Juillion, R. Coquet, J.F. Fontaine, Methodology for the assessment of measuring uncertainties of articulated arm coordinate measuring machines, *Meas Sci Technol*, 25 (2014).
- [5] H. Kevin, *Handbook of Optical Dimensional Metrology*, Taylor & Francis 2013.
- [6] R. Furferi, L. Governi, Y. Volpe, M. Carfagni, Design and Assessment of a Machine Vision System for Automatic Vehicle Wheel Alignment, *Int J Adv Robot Syst*, 10 (2013).
- [7] Creaform, HandyPROBE Next™, accessed, 21 April 2017, <https://www.creaform3d.com/en/metrology-solutions/coordinate-measuring-machines-handyprobe>
- [8] GOM, GOM Touch Probe, accessed, 21 April 2017, <http://www.gom.com/metrology-systems/system-overview/gom-touch-probe.html>
- [9] Leica, Leica T-Probe, accessed, 21 April 2017, <http://www.exactmetrology.com/metrology-equipment/leica-geosystems/t-probe>
- [10] S. Barone, A. Paoli, A.V. Razonale, Multiple alignments of range maps by active stereo imaging and global marker framing, *Optics and Lasers in Engineering*, 51 (2013) 116-127.
- [11] D. Traghella, A. Paoli, S. Barone, A.V. Razonale, Multi-Sensor Reverse Engineering Technique for the Acquisition of Centrifugal Pump Impellers, *International Design Engineering Technical Conferences and Computers and Information in Engineering Conference*, ASME, Boston, Massachusetts, USA, 2015, pp. V02BT03A018.
- [12] S. Barone, A. Paoli, A.V. Razonale, Optical Tracking of a Tactile Probe for the Reverse Engineering of Industrial Impellers, *J Comput Inf Sci Eng*, (2017) in press, doi: 10.1115/1.1111.4036119.